sustainability

MDPI

Article

Microbially Induced Calcite Precipitation (MICP) for Stabilization of Desert Sand against the Wind-induced Erosion: A Parametric Study

Lei Hang [1], Enjie Yang [2], Yundong Zhou [1], Wenzhi Song [3] and Jia He [1,*]

[1] Key Laboratory of Geomechanics and Embankment Engineering of Ministry of Education, Hohai University, Nanjing 210024, China
[2] China Energy Engineering Group Zhe Jiang Electric Power Design Institute Co., Ltd., Hangzhou 310000, China
[3] Shanghai MCC20 Construction Corporation Limited, Shanghai 201999, China
* Correspondence: hejia@hhu.edu.cn; Tel.: +86-15205196646

Abstract: Biocementation, based on microbially induced calcite precipitation (MICP), is a novel soil improvement method, which can form a cemented layer on the surface of desert sand to resist wind-induced erosion. In this work, the surface penetration resistance test and wind tunnel test were conducted to evaluate the various influential factors for the resistance of biocemented desert sand to wind-induced erosion, including the treatment factors, such as treatment temperature and biocement solution concentration, and durability factors such as the development of time, freezing–thawing cycles, and drying–wetting cycles. The test results demonstrated that the erosion resistance of biocemented desert sand was improved by the increase of treatment temperature and the concentration of biocement solution, which was manifested in the increase of surface penetration resistance of biocemented samples. In addition, the resistance of biocemented desert sand to wind-induced erosion decreased with the increased number of drying–wetting cycles, to lesser extents, with the development of time and the increased number of freezing–thawing cycles.

Keywords: microbially induced calcite precipitation; desert sand; wind-induced erosion; surface penetration resistance test; wind tunnel test

Citation: Hang, L.; Yang, E.; Zhou, Y.; Song, W.; He, J. Microbially Induced Calcite Precipitation (MICP) for Stabilization of Desert Sand against the Wind-induced Erosion: A Parametric Study. *Sustainability* **2022**, *14*, 11409. https://doi.org/10.3390/su141811409

Academic Editors: Ning Zhang, Shuai Li, Denghui Dai and Xin Chen

Received: 3 August 2022
Accepted: 6 September 2022
Published: 11 September 2022

1. Introduction

Land desertification is one of the most serious environmental problems in the world, which poses an enormous threat to national economic development, social stability, and ecological balance [1]. Wind-induced erosion as a major cause of desertification and sandstorm in arid and semi-arid areas, decreases the fine-grained contents of soil particles and nutrients required for plant growth, decreasing the water-retaining capacity and soil fertility [2]. Meanwhile, the dust suspended in the atmosphere is transported away from the local region with the blowing wind, which obscures visibility, pollutes the air, and endangers human health [3]. Due to the consideration of agriculture, environment, and human health, it is imperative to control the wind-induced erosion of sandy soil in arid and semi-arid areas.

Over the past few decades, various approaches, such as vegetation and chemical solidification, have been employed to minimize the wind-induced erosion. The vegetation cover on the land surface is one of the effective methods to prevent the wind erode the surface of sandy soils, and the greater the vegetation cover is, the more effective it would be [4]. However, the vegetation methods may be difficult in some areas where soils are agriculturally unsuitable, and the strong winds tend to uproot seeding or bury them with drifting sand [5]. In the case of potential failure to establish the vegetation, chemical solidification methods could be used [6,7]. As for the chemical modification of soils, various inorganic and organic materials such as cements, petroleum products, and synthetic

polymers can be used as stabilizers [8–10]. These stabilizers can immobilize sandy soils from being eroded by the wind. However, some of the chemical soil stabilizers may be toxic and/or hazardous and can create environmental pollution [11,12].

In recent years, biocementation based on microbially induced calcium carbonate precipitation (MICP) using the urea hydrolyzing process, was adopted as a novel soil enhancement method to upgrade the mechanical properties of the soil. This method can be described in two reaction steps. First, urea is hydrolyzed into ammonium and carbonate using *Sporosarcina pasteurii*, which is a ureolytic bacteria. Secondly, the produced carbonate precipitates as calcium carbonate minerals with a source of calcium. The reactions proceed as follows:

$$NH_2-CO-NH_2 + 2H_2O \overset{\text{ureolytic bacteria}}{\rightarrow} 2NH_4{}^{+} + CO_3{}^{2-} \quad (1)$$

$$Ca^{2+} + CO_3{}^{2-} \rightarrow CaCO_3 \downarrow . \quad (2)$$

When calcium carbonate is formed in the soil pores, it binds the soil particles by acting as a cementing agent and fills the soil pores. Thereby, the strength and the stiffness of the soils were improved [13–18]. Further, the biocement method was employed to solve various geotechnical problems, which include the liquefiable grounds enhancement, foundation bearing capacity, and slope stability [19–25]. Comparing with the untreated pile foundation [26], research show that the reinforcement pile foundation using biocement method can effectively improve the bearing capacity [27].

Additionally, some researchers have also reported the effectiveness of MICP method in strengthening the wind-induced erosion resistance of sandy soils [28–30]. However, most of the previous studies only focused on assessing the effectiveness of biocementation in resisting the wind-induced erosion of sandy soils; ignoring the biocemented sand would be subjected to long-term complex environmental challenges under natural conditions. The challenges include the drying–wetting cycles and freezing–thawing cycles resulting from rainfall, snowfall, and temperature variation. The strength of biocemented layers may also change with the development of time. Besides, the reinforcement effect of biocementation on soils is also affected by treatment conditions. Therefore, the objective of this study is to investigate various influential factors for the resistance of biocemented desert sand to wind-induced erosion, including the treatment factors such as treatment temperature and biocement solution concentration, and durability factors such as the development of time, freezing–thawing cycles and drying–wetting cycles.

2. Materials and Methods

2.1. Desert Sand

Desert sand was collected from the southwestern fringe of Ulan Buh Desert, Ningxia Hui Autonomous Region, China. Table 1 presents the basic properties of the desert sand. The grain size distribution of desert sand is shown in Figure 1.

2.2. Biocementation

As mentioned above, the biocementation is based on a urea hydrolyzing process mediated by ureolytic bacteria. Therefore, the microbial treatment was carried out using urea, calcium salt, and ureolytic bacteria.

Table 1. Basic properties of desert sand.

Property	Value
Specific Gravity, G_s	2.64
Uniformity coefficient, C_u	1.93
Coefficient of curvature, C_c	0.84
Maximum void ratio, e_{max}	0.942
Minimum void ratio, e_{min}	0.436

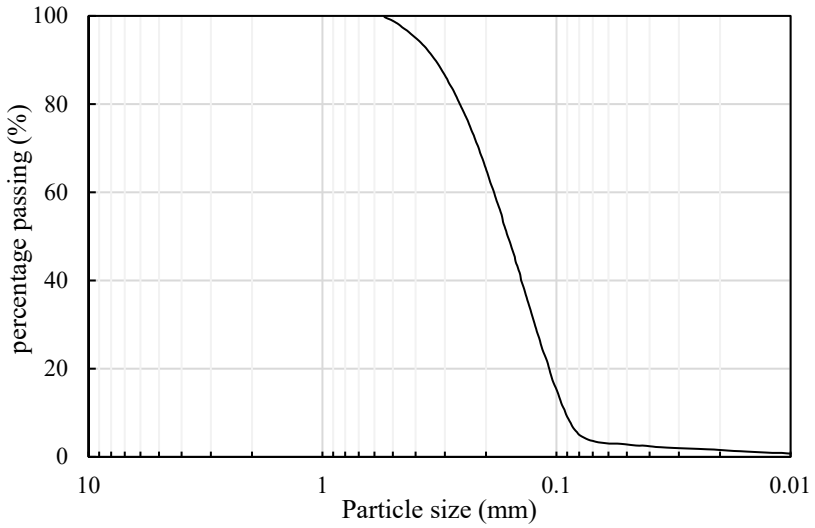

Figure 1. Grain size distribution of desert sand.

2.2.1. Cultivation of Bacteria

In this work, *Sporosarcina pasteurii* (CGMCC1.3687) was employed for the microbial treatment. The bacteria are halotolerant and have a high capability to hydrolyze urea into ammonium and carbonate. The bacteria were grown in a liquid medium, which consists of 20 g/L of yeast extract, 10 g/L NH_4Cl, 0.024 g/L $NiCl_2{\cdot}6H_2O$, 0.01 g/L $MnSO_4{\cdot}H_2O$, and 2 mol/L NaOH solution to adjust the pH level between 8.5 and 9.0. Further, before inoculation, the liquid medium was autoclaved. The bacteria were grown in a shaking incubator at 30 °C and 120 rotations-per-minute under aerobic conditions for approximately 1 day. The harvested bacteria were diluted with 0.9% sodium chloride to a urase activity of 7.5−8 mM-urea/min (7.5–8 mM urea hydrolyzed per minute) [31,32], and the bacteria were used instantly after harvesting.

2.2.2. Cultivation of Bacteria

A bacterial suspension was mixed with a urea–calcium chloride solution (1:1 volume ratio) in order to obtain the biocement solution. Three concentrations of biocement solution were used, namely 0.1 M, 0.2 M, and 0.4 M. Herein, the concentration values refer to the concentrations of calcium chloride in the biocement solution. The concentration of urea is 1.5 times of calcium chloride in the biocement solution. The sand was sprayed with the biocement solution instantly after mixing.

2.3. Sample Preparation and Microbial Treatment

Thirty-eight pans of desert sand were prepared at the bulk density for the following tests, where two pans of sand were untreated as the reference. A list of the test parameters and brief results is given in Table 2. To note that, duplicate soil samples for each test number were prepared for conducting the wind-blown sand erosion test and for measuring the surface penetration resistance and the $CaCO_3$ content. The soil samples were prepared with the following procedure:

- Initially, pre-weighed desert sand was loosely filled into the stainless-steel pan (24 × 17 × 4 cm) to attain a bulk density at 1.47 g/cm^3;
- Further, the prepared bacteria, urea–calcium chloride solution and the desert sand were placed in a thermostatic curing box to reach the designed temperature;
- Thereafter, the bacterial suspension was mixed with the urea–calcium chloride solution (1:1 volume ratio) to obtain the biocement solution, which was sprayed evenly on the sand surface with 4 L/m^2 at a rate of 3.33 mL/s;
- Then, the samples were placed in the thermostatic curing box for three days to ensure a maximum reaction for multiphase MICP-treated soils;

- After curing, the samples were oven-dried at 60 °C until no change in mass was observed.

Table 2. Testing parameters and brief test results.

Test no.	Tempereture, (°C)	Biocement Solution Concentration, (mol/L)	Initial Penetration Resistance, (kPa)	Final Penetration Resistance, (kPa)	Initial Wind Erosion, (g)	Finial Wind Erosion, (g)	Calcite Content, (g/m^2)
R-0	30	0	0	-	-	-	0
T-1	10	0.2	115	65	0	0	28
T-2	20	0.2	215	152	0	0	49
T-3	30	0.2	246	168	0	0	59
T-4	40	0.2	271	183	0	0	64
T-5	30	0.1	162	141	0	0	32
T-6	30	0.4	398	291	0	0	99
DW-1	10	0.2	166	96	0	14	32
DW-2	20	0.2	216	131	0	9	50
DW-3	30	0.2	250	165	0	0	58
DW-4	40	0.2	265	206	0	0	62
DW-5	30	0.1	177	74	0	28	34
DW-6	30	0.4	295	205	0	0	69
FT-1	10	0.2	110	33	0	13	27
FT-2	20	0.2	203	108	0	0	47
FT-3	30	0.2	240	140	0	0	57
FT-4	40	0.2	319	211	0	0	74
FT-5	30	0.1	193	90	0	0	36
FT-6	30	0.4	360	278	0	0	86

Note: Except for sample R-0, the name of a test consists of two parts: durability factors and the sample ID, 'T' for Time, 'DW' for drying–wetting cycles, 'FT' for freezing–thawing cycles. As for sample R-0, 'R' means reference, and '0' is sample ID.

When the samples were prepared, wind tunnel test and surface penetration test were carried out immediately (denoted as day 0), day 3, day 7, day 14, day 28, and day 56 to study the variation of sample surface stability with the development of time. In the freezing–thawing cycle process, the cured samples were placed in a refrigerator at −20 °C for 12 h, then thawed at room temperature of approximately 20 °C for 12 h, and then dried at 60 °C. This process was recorded as one freezing–thawing cycle. Wind tunnel test and surface penetration test were performed before the freezing–thawing cycle and after the 1st, 2nd, 3rd, 5th, 7th, and 10th freezing–thawing cycles, respectively. In the drying–wetting cycle process, 250 mL deionized water was uniformly sprayed on the surface of the samples, and dried at 60 °C after 24 h. This process was recorded as one drying–wetting cycle. Wind tunnel test and surface penetration test were conducted before the drying–wetting cycle and after the 1st, 2nd, 3rd, 5th, and 7th drying–wetting cycles, respectively.

2.4. Wind Tunnel Test and Surface Penetration Resistance Test

A wind tunnel equipment was utilized to conduct the wind tunnel test (Figure 2). The testing wind velocity was 15 m/s, and the duration was 10 min. The mass of these samples was measured before and after the wind tunnel test, and the difference in mass was the amount of erosion of these samples.

The penetrometer test has been anther indirect method used in recent years to assess the wind-induced erosion resistance of soil surface [33,34]. A micro-penetrometer (*HP-50*, *Aidebao*, China) with a diameter of 6 mm was adopted to measure the surface penetration resistance of these samples in this study (Figure 3). The micro-penetrometer was penetrated over nine randomly selected points on oven-dried soil specimens, and the maximum force was recorded. The surface penetration resistance was averaged by seven of the five recorded values, discarding the maximum and the minimum ones.

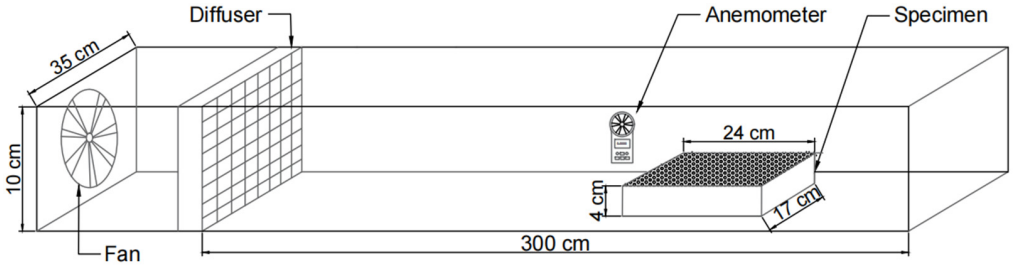

Figure 2. Schematic diagram of the wind tunnel equipment.

Figure 3. The wind tunnel equipment.

2.5. Calcium Carbonate Content Measurement

Nine small pieces of sand in the crust with a thickness of about 15 mm were taken from different positions at the soil surface after the surface penetration test to measure the $CaCO_3$ content in each sample surface. During this process, a small quantity of sand was rinsed in deionized water and mixed with an appropriate quantity of acidic liquid to promote the dissolution of the calcium carbonate. Further, the EDTA titrimetric method was employed to measure the calcium concentration in the acidic liquid [35]. Thereafter, the calcium carbonate content in each sample surface was determined (Table 2).

3. Results and Discussion

3.1. The Influence of the Treatment Factors

3.1.1. Effects of Treatment Temperature

Figure 4 shows the variation of surface penetration resistance and calcium carbonate content of the MICP treated samples with different treatment temperatures. In general, the surface penetration resistance of the MICP treated samples increases with the increasing treatment temperature, which indicates the surface stabilization effect of MICP on desert sand increases with the increase in treatment temperature. This is similar to that observation obtained by Bang et al. (2011) [36]. They demonstrated that the wind erosion resistance of biocemented soil samples increased with the elevated temperature (20 °C, 35 °C, and 45 °C). From Figure 4 and Table 2, it is observed that an increase in the treatment temperature from 10 °C to 40 °C at the concentration of biocement solution 0.2 mol/L enhances the average surface penetration resistance of the reinforced layers from 130 kPa to 285 kPa after MICP treatment, while the surface penetration resistance of the untreated sample is 0. The general trend of the surface penetration resistance of MICP treated samples-treatment temperature behavior could be explained by the vibration of calcium carbonate content with treatment temperature in the biocememented layers. As the treatment temperature increases from 10 °C to 40 °C, the average calcium carbonate content in the biocemented layers increases

from 29 g/m^2 to 67 g/m^2. In this study, under the condition of the same biocement solution formula, the increase in temperature increases the conversion of calcium ions in the reaction, thereby increasing the production of calcium carbonate in the biocemented soil. In biocemented soils, the produced calcium carbonate can bind soil particles and fill soil pores to improve soil strength and integrity. This improvement effect could be enhanced by an increase in calcium carbonate content. Therefore, the higher amount of calcium carbonate results in a higher surface penetration resistance of the biocemented desert sand. In the wind tunnel test, the biocemented samples have no mass loss at any temperature, while the sand of untreated sample is basically blown out, which suggests the improvement effect of biocementation on the wind-induced erosion resistance of desert sand.

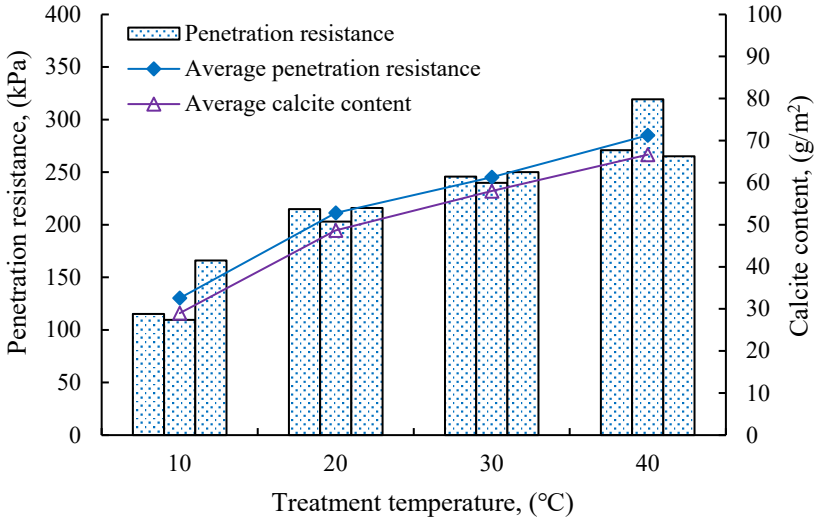

Figure 4. Surface penetration resistance and calcium carbonate content of MICP-treated desert sand at various treatment temperatures.

3.1.2. Effects of the Biocement Solution Concentration

The surface penetration resistance and the calcium carbonate content of the MICP-treated desert sand with different concentrations of biocement solution are plotted in Figure 5. For soil samples at a varying concentration of biocement solution, the average surface penetration resistance increases from 177 kPa to 254 kPa, as the concentration of biocement solution increases from 0.1 mol/L to 0.2 mol/L, and it increases to 351 kPa as the concentration of biocement solution keep increasing to 0.4 mol/L. From Figure 5 and Table 2, it is observed that when the concentration of biocement solution increases from 0.1 mol/L to 0.2 mol/L, and the average calcium carbonate content in the biocemented layers increases from 34 g/m^2 to 58 g/m^2. Further, as the concentration of biocement solution increases to 0.4 mol/L, the average calcium carbonate content reaches 85 g/m^2. In the range of the biocement solution concentrations herein, the higher concentration of the biocement solution provides more reactants in the biocementation reaction, leading to more calcium carbonate generated in the soils, thereby enhancing the surface penetration resistance of the sample. In addition, there is no mass loss of soil at any concentration of biocement solution, which indicates that although the average surface penetration resistance of the biocemented desert sand with the lowest biocement solution 0.1 mol/L is only about 177 kPa, it also achieves the effect of resisting the wind-induced erosion.

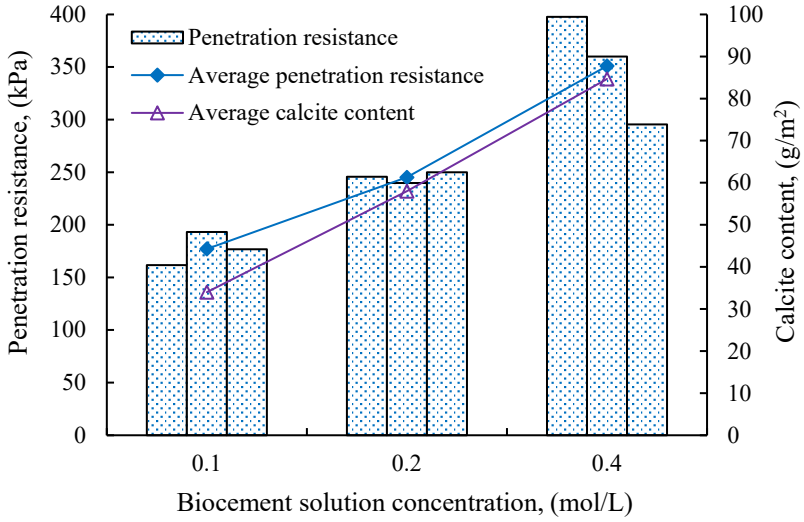

Figure 5. Surface penetration resistance and calcium carbonate content of MICP-treated desert sand at various concentrations of biocement solution.

3.2. The Influence of Durability Factors

3.2.1. Effects of the Development of Time

The surface penetration resistance of the MICP-treated desert sand is plotted for the two groups in Figure 6. In general, the surface penetration resistance of soil samples decreases with the development of time. Moreover, the attenuation of the surface penetration resistance of soil samples mainly occurs in the first 28 days, and the attenuation rate of the surface penetration resistance slows down with the development of time. The bacteria used in this study are bacterial fluids without centrifugation, so there is a certain amount of organic matter components in the biocement solution. The surface penetration resistance of soil samples treated with the biocement solution derives not only from the cementation of the produced calcium carbonate, but also partly from the bonding of organic matter and residual salt. However, the organic matter gradually decomposes with the development of time, and the surface penetration resistance provided by the organic matter is gently lost, so the penetration resistance of the MICP-treated soil samples decreases. After the organic matter completely decomposes, the surface penetration resistance provided by the organic matter disappears, and the penetration resistance of the MICP-treated samples tends to be stable. Some of the anomalies in Figure 6, where the resistance increases with time or decreases too much with time, may be due to the deviations caused by uneven local biocement treatment. Table 2 shows that the cumulative mass loss of the MICP-treated desert sand is 0 in the wind tunnel test, which implies that the remaining strength is also enough to resist the wind erosion of 15 m/s, despite the decomposition of organic matter resulting in a certain decrease in the surface penetration strength.

3.2.2. Effects of Freezing and Thawing Cycles

Figure 7 shows the relationship between the surface penetration resistance and the number of freezing and thawing cycles for the two test groups of MICP-treated desert sand. It is observed that as the number of freezing and thawing cycles increases, the overall trend of the surface penetration resistance of MICP-treated desert sand decreases, and the adverse effect of the freezing–thawing cycles is gradually weakened. For example, the surface penetration resistance of sample FT-3 decreases from 240 kPa to 178 kPa after five freezing–thawing cycles, which is reduced by 24%. After ten freezing–thawing cycles, its surface penetration resistance is 140 kPa, which decreases by 42% compared with the initial surface strength. Thus, the reduction rate of the initial surface strength of sample FT-3 is 18% in the last five freezing–thawing cycles, which is smaller than 24% in the first five freezing–thawing cycles. It is worth noting that some of the anomalies in Figure 7

may also result from the deviations caused by uneven local biocement treatment, which is similar with Figure 6. There are two reasons for the surface penetration resistance of MICP-treated desert sands decreasing with the increasing number of freezing–thawing cycles. The first is the organic matter that decomposes with the development of time. The second is the dissolution and migration of salt caused by the condensation of water vapor on the surface of the samples during the freezing–thawing cycles. Further, the decomposition of organic matter and the dissolution and migration of salt weakens the bonding effect of calcium carbonate. Therefore, after ten freezing–thawing cycles, sample FT-1 with the lowest calcium carbonate content had a soil erosion of 13 g in the wind tunnel test, while the soil erosion of other samples is 0.

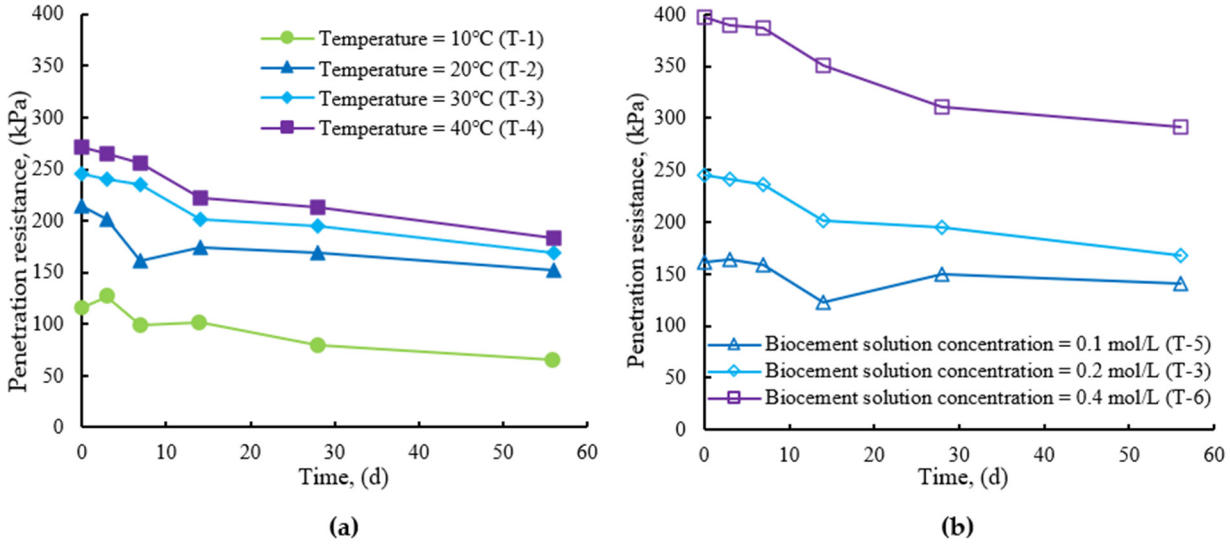

Figure 6. The relationship between surface penetration resistance of MICP-treated desert sand and time: (**a**) samples with different treatment temperatures; (**b**) samples with different concentrations of biocement solution.

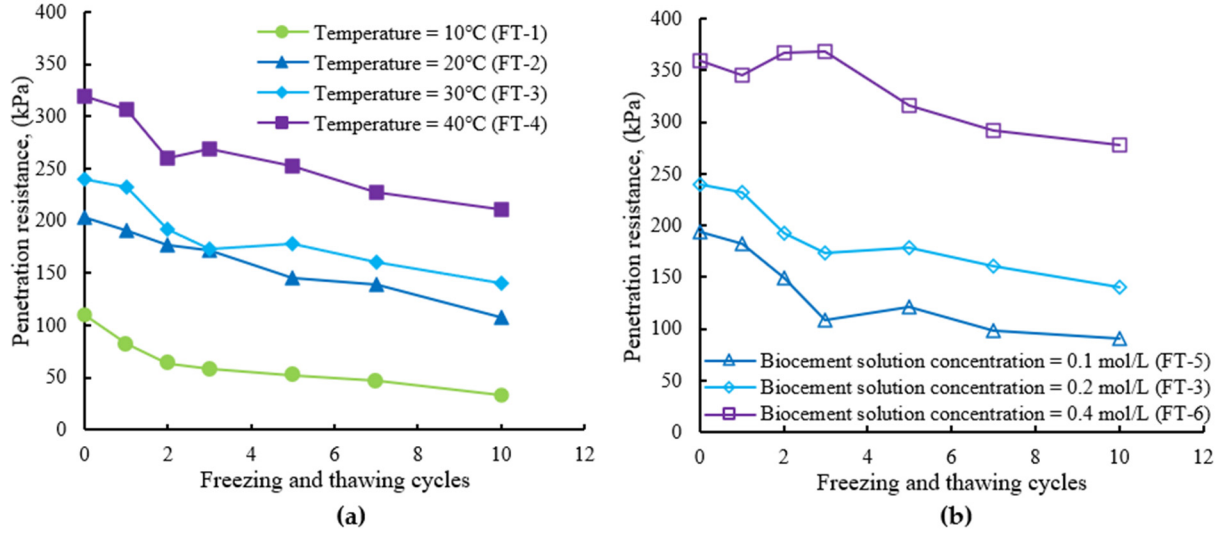

Figure 7. The relationship between penetration resistance of MICP-treated desert sand and number of freezing–thawing cycles: (**a**) samples with different treatment temperatures; (**b**) samples with different concentrations of biocement solution.

3.2.3. Effects of Drying and Wetting Cycles

Figure 8 plots the surface penetration resistance versus number of drying and wetting cycles for the two test groups of the MICP-treated desert sand. For the biocemented samples treated at any temperature and concentration of biocement solution, the increase in the number of drying-wetting cycles decreases their surface penetration resistance. For most of the MICP-treated samples, the strength reduction mainly occurs in the first three drying–wetting cycles, and then the strength reduction rate slows down with the increase in the number of drying–wetting cycles. For instance, the surface penetration resistance of sample DW-2 reduces from 216 kPa to 165 kPa after three drying–wetting cycles, and the strength is reduced by 24%. However, the reduction rate of the initial surface strength of sample DW-2 is 15% in the last four drying–wetting cycles, which is smaller than 24% in the first three drying–wetting cycles. After the end of seven drying–wetting cycles, it is also found that floating sand appears on the surface of some samples (samples DW-1, DW-2 and DW-5). Therefore, in the wind tunnel test, the mass loss of samples DW-1, DW-2, and DW-5 is 14 g, 9 g, and 28 g, respectively. The reduction of the strength of all samples and the wind erosion of some samples after seven drying–wetting cycles result from the dissolution, loss of organic matter, and residual salt in the biocemented desert sand. Moreover, the migration of residual salt caused by the drying–wetting cycle further weakens the bonding effect of calcium carbonate on the soil. In this work, compared with the freezing–thawing cycles, the drying–wetting cycles have more serious damage to the wind erosion resistance of the MICP-treated samples. For the biocemented samples treated at the same treatment conditions, after experiencing the same number of drying–wetting cycles or freezing–thawing cycles, the strength of the sample after experiencing the drying–wetting cycles is reduced more. For example, the strength reduction rate of sample DW-2 is 39% after seven drying–wetting cycles, and the strength reduction rate of sample FT-2 is 32% after seven freezing–thawing cycles. The main reason for this phenomenon is that during the drying–wetting cycles, the moisture in the sample changes more, the dissolution and migration of organic matter and salt are more obvious, and the bonding effect of the calcium carbonate is weakened more.

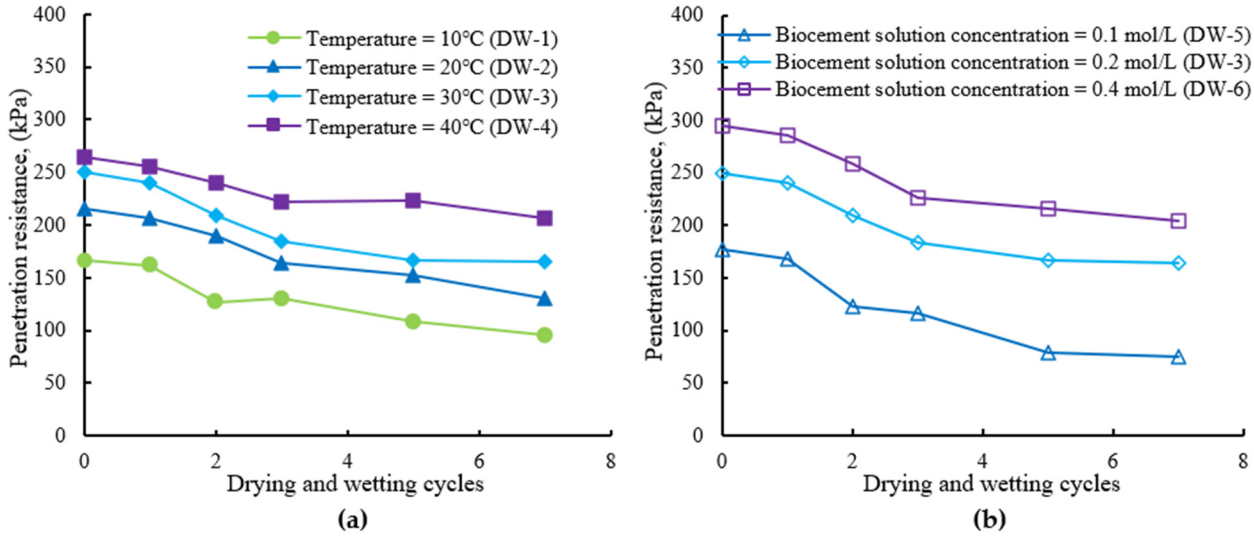

Figure 8. The relationship between penetration resistance of MICP-treated desert sand and number of drying–wetting cycles: (**a**) samples with different treatment temperatures; (**b**) samples with different concentrations of biocement solution.

4. Conclusions

In this paper, several laboratory tests were performed to study the influences of different factors on the wind-induced erosion resistance of biocemented desert sand. The various influential factors include the treatment factors such as treatment temperature and

biocement solution concentration, and durability factors such as the development of time, freezing–thawing cycles, and drying–wetting cycles. Based on the experimental results, the conclusions are arrived at as follows:

The MICP method could effectively reduce the erosion potential of desert sand subjected to wind. Test results demonstrated that the surface penetration resistance of MICP-treated samples was enough to resist the wind erosion of 15 m/s (the soil erosion of biocemented samples was 0), while the sand of untreated sample was basically blown out (the surface penetration resistance of untreated sample was 0);

The surface penetration resistance of MICP-treated desert sand increased for increasing the treatment temperature and the concentration of biocement solution, which implied that the resistance to wind-induced erosion is enhanced. The increase in the treatment temperature and the higher concentration of biocement solution could improve the calcium carbonate content in the biocemented layers, which could more effectively strengthen the bonding effect of calcium carbonate on the soils.

The resistance of biocemented desert sand to wind-induced erosion decreased with the increased number of drying–wetting cycles, to a lesser extent with the development of time and the increased number of freezing–thawing cycles. The weakening effect of these three durability factors on the wind erosion resistance of biocemented samples mainly resulted from the decomposition of organic matter and the dissolution and migration of salt, and the weakening effect decreased with the progress of each test.

Author Contributions: Conceptualization, L.H. and J.H.; methodology, L.H., E.Y., J.H. and W.S.; validation, L.H., Y.Z. and J.H.; formal analysis, E.Y., W.S. and Y.Z.; investigation, L.H., E.Y., Y.Z. and W.S.; resources, L.H. and J.H.; data curation, and L.H.; writing—original draft preparation, E.Y.; writing—review and editing, L.H. and J.H.; visualization, E.Y.; supervision, L.H.; project administration, L.H., J.H. and W.S.; funding acquisition, L.H., J.H. and Y.Z. All authors have read and agreed to the published version of the manuscript.

Funding: This research was funded by the National Natural Science Foundation of China, grant numbers 51979088.

Institutional Review Board Statement: Not applicable.

Informed Consent Statement: Not applicable.

Data Availability Statement: The data presented in this study are available on request from the corresponding author.

Conflicts of Interest: The authors declare no conflict of interest. The funders had no role in the design of the study; in the collection, analyses, or interpretation of data; in the writing of the manuscript; or in the decision to publish the results.

References

1. Jiang, L.L.; Jiapaer, G.; Bao, A.M.; Kurban, A.; Guo, H.; Zheng, G.X.; De Maeyer, P. Monitoring the long-term desertification process and assessing the relative roles of its drivers in Central Asia. *Ecol. Indic.* **2019**, *104*, 195–208. [CrossRef]
2. Kheirabadi, H.; Mahmoodabadi, M.; Jalali, N.H. Sediment flux, wind erosion and net erosion influenced by soil bed length, wind velocity and aggregate size distribution. *Geoderma* **2018**, *323*, 22–30. [CrossRef]
3. Shepherd, G.; Terradellas, E.; Baklanov, A.; Kang, U.; Cha, J. *Global Assessment of Sand and Dust Storms*; UN Environment Programme: Nairobi, Kenya, 2016.
4. Lan, S.B.; Zhang, Q.Y.; Wu, L.; Liu, Y.D.; Zhang, D.L.; Hu, C.X. Artificially accelerating the reversal of desertification: Cyanobacterial inoculation facilitates the succession of vegetation communities. *Environ. Sci. Technol.* **2013**, *48*, 307–315. [CrossRef]
5. Maleki, M.; Ebrahimi, S.; Asadzadeh, F.; Tabrizi, M.E. Performance of microbial-induced carbonate precipitation on wind erosion control of sandy soil. *Int. J. Environ. Sci. Technol.* **2016**, *13*, 937–944. [CrossRef]
6. Ma, R.; Li, J.R.; Ma, Y.J.; Shan, L.S.; Li, X.L.; Wei, L.Y. A wind tunnel study of the airflow field and shelter efficiency of mixed windbreaks. *Aeolian Res.* **2019**, *41*, 100544. [CrossRef]
7. Ma, G.F.; Ran, F.T.; Feng, E.K.; Dong, Z.B.; Lei, Z.Q. Effectiveness of an eco-friendly polymer composite sand-fixing agent on sand fixation. *Water Air Soil Poll.* **2015**, *226*, 221. [CrossRef]
8. Indraratna, B.; Muttuvel, T.; Khabbaz, H.; Armstrong, R. Predicting the erosion rate of chemically treated soil using a process simulation apparatus for internal crack erosion. *J. Geotech. Geoenviron. Eng.* **2008**, *134*, 837–844. [CrossRef]

9. Tang, Q.; Shi, P.X.; Zhang, Y.; Liu, W.; Chen, L. Strength and deformation properties of fiber and cement reinforced heavy metal-contaminated synthetic soils. *Adv. Mater. Sci. Eng.* **2019**, *2019*, 5746315. [CrossRef]
10. Tang, Q.; Zhang, Y.; Gao, Y.F.; Gu, F. Use of cement-chelated solidified MSWI fly ash for pavement material: Mechanical and environmental evaluations. *Can. Geotech. J.* **2017**, *54*, 1553–1566. [CrossRef]
11. Wu, X.; Zou, X.; Zhou, N.; Zhang, C.; Shi, S. Deceleration efficiencies of shrub windbreaks in a wind tunnel. *Aeolian Res.* **2015**, *16*, 11–23. [CrossRef]
12. Lo, C.Y.; Tirkolaei, H.K.; Hua, M.; De Rosa, I.M.; Carlson, L.; Kavazanjian, E.; He, X. Durable and ductile double-network material for dust control. *Geoderma* **2020**, *361*, 114090. [CrossRef]
13. Van Paassen, L.A.; Ghose, R.; van der Linden, T.J.; van der Star, W.R.; van Loosdrecht, M.C. Quantifying biomediated ground improvement by ureolysis: Large-scale biogrout experiment. *J. Geotech. Geoenviron. Eng.* **2010**, *136*, 1721–1728. [CrossRef]
14. DeJong, J.T.; Mortensen, B.M.; Martinez, B.C.; Nelson, D.C. Bio-mediated soil improvement. *Ecol. Eng.* **2010**, *36*, 197–210. [CrossRef]
15. Chu, J.; Stabnikov, V.; Ivanov, V. Microbially induced calcium carbonate precipitation on surface or in the bulk of soil. *Geomicrobiol. J.* **2012**, *29*, 544–549. [CrossRef]
16. Gao, Y.F.; Hang, L.; He, J.; Chu, J. Mechanical behaviour of biocemented sands at various treatment levels and relative densities. *Acta Geotech.* **2019**, *14*, 697–707. [CrossRef]
17. Cardoso, R.; Pedreira, R.; Duarte, S.; Monteiro, G.A. About calcium carbonate precipitation on sand biocementation. *Eng. Geol.* **2020**, *271*, 105612. [CrossRef]
18. Cui, M.J.; Lai, H.J.; Hoang, T.; Chu, J. One-phase-low-pH enzyme induced carbonate precipitation (EICP) method for soil improvement. *Acta Geotech.* **2020**, *9*, 481–489. [CrossRef]
19. Whiffin, V.S.; Van Paassen, L.A.; Harkes, M.P. Microbial carbonate precipitation as a soil improvement technique. *Geomicrobiol. J.* **2007**, *24*, 417–423. [CrossRef]
20. Chu, J.; Ivanov, V.; Naeimi, M.; Stabnikov, V.; Liu, H.L. Optimization of calcium-based bioclogging and biocementation of sand. *Acta Geotech.* **2014**, *9*, 277–285. [CrossRef]
21. Salifu, E.; MacLachlan, E.; Iyer, K.R.; Knapp, C.W.; Tarantino, A. Application of microbially induced calcite precipitation in erosion mitigation and stabilization of sandy soil foreshore slopes: A preliminary investigation. *Eng. Geol.* **2016**, *201*, 96–105. [CrossRef]
22. Hang, L.; Gao, Y.F.; He, J.; Chu, J. Mechanical behavior of biocemented sand under triaxial consolidated undrained or constant shear drained conditions. *Geomech. Eng.* **2019**, *17*, 497–505.
23. Wu, C.; Chu, J.; Wu, S.; Hong, Y. 3D characterization of microbially induced carbonate precipitation in rock fracture and the resulted permeability reduction. *Eng. Geol.* **2019**, *249*, 23–30. [CrossRef]
24. Liu, B.; Zhu, C.; Tang, C.S.; Xie, Y.H.; Yin, L.Y.; Cheng, Q.; Shi, B. Bio-remediation of desiccation cracking in clayey soils through microbially induced calcite precipitation (MICP). *Eng. Geol.* **2020**, *264*, 105389. [CrossRef]
25. Tang, Q.; Gu, F.; Zhang, Y.; Zhang, Y.Q.; Mo, J.L. Impact of biological clogging on the barrier performance of landfill liners. *J. Environ. Manag.* **2018**, *222*, 44–53. [CrossRef] [PubMed]
26. Dai, D.; El Naggar, M.H.; Zhang, N.; Wang, Z. Rigorous solution for kinematic response of floating piles subjected to vertical P-wave. *Appl. Math. Model.* **2022**, *106*, 114–125. [CrossRef]
27. He, R.; Wang, H.; Zheng, J. Influence of MICP reinforcement on static properties of monopiles of offshore wind turbine. *J. Hohai Univ.* **2022**, *50*, 65–73.
28. Anderson, J.; Bang, S.; Bang, S.S.; Lee, S.J.; Choi, S.R.; Dho, N.Y. Reduction of wind erosion potential using microbial calcite and soil fibers. In Proceedings of the Geo-Congress 2014: Geo-characterization and Modeling for Sustainability, Atlanta, Georgia, 23–26 February 2014.
29. Nikseresht, F.; Landi, A.; Sayyad, G.; Ghezelbash, G.; Schulin, R. Sugarecane molasse and vinasse added as microbial growth substrates increase calcium carbonate content, surface stability and resistance against wind erosion of desert soils. *J. Environ. Manag.* **2020**, *268*, 110639. [CrossRef]
30. Woolley, M.A.; van Paassen, L.A.; Kavazanjian, E. Impact on surface hydraulic conductivity of EICP treatment for fugitive dust mitigation. In Proceedings of the Geo-Congress, Minneapolis, MN, USA, 25–28 February 2020.
31. Whiffin, V.S. Microbial $CaCO_3$ precipitation for the production of biocement. Ph.D. Dissertation, Murdoch University, Perth, Australia, 2004.
32. Van Paassen, L.A. Biogrout Ground Improvement by Microbially Induce Carbonate Precipitation. Ph.D. Thesis, Delft University of Technology, Delft, The Netherlands, 2009.
33. Chen, R.; Lee, I.; Zhang, L. Biopolymer stabilization of mine tailings for dust control. *J. Geotech. Geoenviron. Eng.* **2014**, *141*, 04014100. [CrossRef]
34. Fattahi, S.M.; Soroush, A.; Huang, N. Biocementation control of sand against wind erosion. *J. Geotech. Geoenviron. Eng.* **2020**, *146*, 04020045. [CrossRef]
35. MOEE. Water Quality-Determination of Calcium -EDTA Titrimetrlc Method. China, GB 7476-87, 1987. Available online: https://std.samr.gov.cn/gb/search/gbDetailed?id=71F772D7B379D3A7E05397BE0A0AB82A (accessed on 5 September 2022).
36. Bang, S.C.; Min, S.H.; Bang, S.S. Application of microbiologically induced soil stabilization technique for dust suppression. *Int. J. Geo-Eng.* **2011**, *3*, 27–37.